Bioorg. Med. Chem. Lett. 44 (2021) 128082

Contents lists available at ScienceDirect

Bioorganic & Medicinal Chemistry Letters

journal homepage: www.elsevier.com/locate/bmcl

Discovery of novel *N*-1 substituted pyrazolopyrimidinones as potent, selective PDE2 inhibitors

Gregori J. Morriello [a,*], Michael P. Dwyer [a], Yili Chen [a], Anthony T. Ginetti [a], Shimin Xu [a], Jun Lu [d], Pravien Abeywickrema [d], Deping Wang [d], Alejandro Crespo [d], Tamara D. Cabalu [b], Jonathan E. Wilson [d], Shawn J. Stachel [d], Daniel V. Paone [d], Christopher Sinz [c]

[a] *Discovery Chemistry, Merck & Co., Inc., 2000 Galloping Hill Rd., Kenilworth, NJ 07033, USA*
[b] *Drug Metabolism, Merck & Co., Inc., 770 Sumneytown Pike, West Point, PA 19486, USA*
[c] *Discovery Chemistry, Merck & Co., Inc., 213 E. Grand Avenue, South San Fransisco, CA 94080, USA*
[d] *Discovery Chemistry, Merck & Co., Inc., 770 Sumneytown Pike, West Point, PA 19486, USA*

ARTICLE INFO

Keywords:
PDE2
cAMP
cGMP
Pyrazolopyrimidinone

ABSTRACT

A focused SAR study was conducted on a series of *N*1-substituted pyrazolopyrimidinone PDE2 inhibitors to reveal compounds with excellent potency and selectivity. The series was derived from previously identified internal leads and designed to enhance steric interactions with key amino acids in the PDE2 binding pocket. Compound **26** was identified as a lead compound with excellent PDE2 selectivity and good physicochemical properties.

Phosphodiesterases (PDE) play a key role in the degradation of secondary messengers 3′,5′- cyclic adenosine monophosphate (cAMP) and 3′,5′-cyclic guanosine monophosphate (cGMP).[1] There are 11 PDE families which have different tissue distribution and possess different selectivity for cAMP and cGMP.[2] Both cAMP and cGMP have been implicated in playing a key role in intracellular signaling, neuronal plasticity, and long-term potentiation which could improve cognitive function and memory.[3–5]

PDE2 is a dual-substrate enzyme which is stimulated by cGMP and which degrades both cAMP and cGMP.[6] PDE2 is highly expressed in the human brain where it is localized in the cortex, hippocampus, and striatum.[7] PDE2 inhibition elevates the levels of these cyclic nucleotides which could enhance cognitive and hippocampal function, which are altered in diseases such as schizophrenia and Alzheimer's disease.[1] Towards this end, there has been a considerable effort to identify selective, brain penetrant PDE2 inhibitors towards the treatment of cognitive disorders.[8] Fig. 1 summarizes some of these compounds; from early compounds, like Bay 60–7550 and TAK-915, to more recent derivatives from Janssen and Pfizer and several reviews have recently covered this area.[9–14]

We had recently disclosed an inhibitor series that was identified via fragment based and high throughput screening.[15] These pyrazolopyrimidinones proved to have good binding affinity to PDE2 and displayed some selectivity over the other PDE members. Herein, we describe a new series of PDE2 inhibitors to which we based the core of the compound on "flipping" the pyrazolopyrimidinone core discovered previously. We describe how we developed chemistry to make the new analogs and how we proceeded to identify a new lead class of compounds for PDE2 inhibition.

While our early work in the PDE2 area focused upon pyrazolopyrimidinone core derivatives of type **A**,[16] one could envisage the idea of a simple flip of the pyrazolo ring would lead to compounds of type **B**. This may engender divergent off-target and pharmacokinetic profiles while maintaining the similar display of critical pharmacophores. The SAR for this series could easily be probed using a combination of *N*-alkylation chemistry (R_2) coupled with a Suzuki coupling strategy to install the requisite α-branching benzylic moiety. This chemistry is well suited for both library and singleton syntheses to push the SAR far more rapidly than the pyrazolopyrimidinones of type **A**.

Initial chemistry efforts focused upon preparation of the *N*1-H and *N*1-methyl substituted core compounds shown in Scheme 1. Treatment of either **1** or **2** with benzyl ethanimidiothioate hydrochloride under basic conditions afforded bicyclic cores **3** or **4** respectively that upon treatment with NBS afforded compounds **5** and **6**. Suzuki coupling with the requisite vinyl boronate in the presence of $Pd(OAc)_2$ and sodium 3,3′,3″- phosphinetriyltribenzenesulfonate hydrate afforded olefins **7**

* Corresponding author.
E-mail address: greg_morriello@merck.com (G.J. Morriello).

https://doi.org/10.1016/j.bmcl.2021.128082
Received 18 December 2020; Received in revised form 23 April 2021; Accepted 28 April 2021
Available online 13 May 2021
0960-894X/© 2021 Elsevier Ltd. All rights reserved.

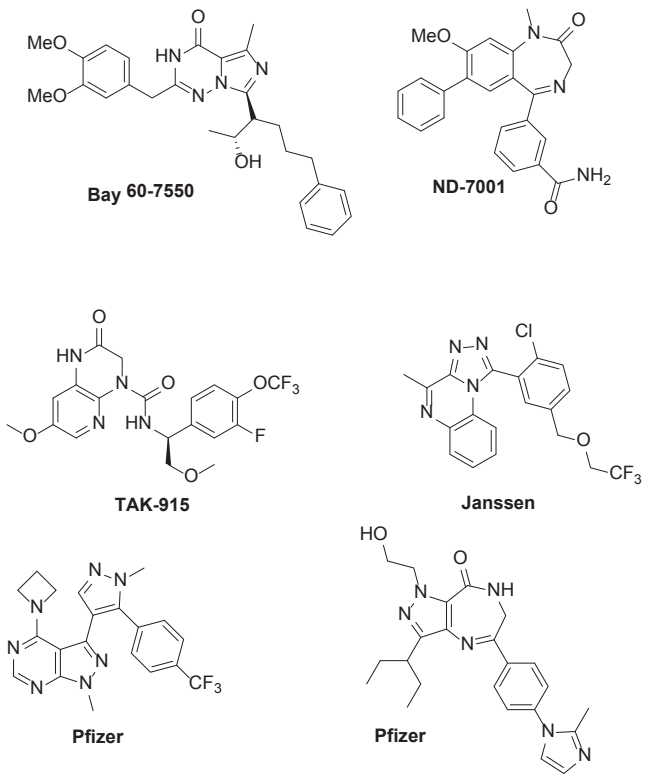

Fig. 1. Reported PDE2 inhibitors.[9–14]

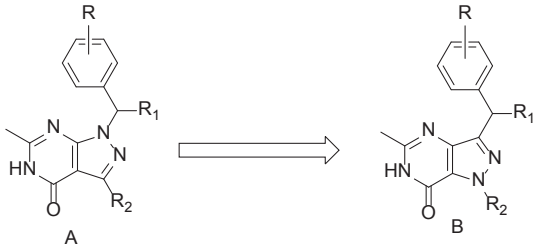

Fig. 2. Markush example of the "flipped" pyrazole ring.

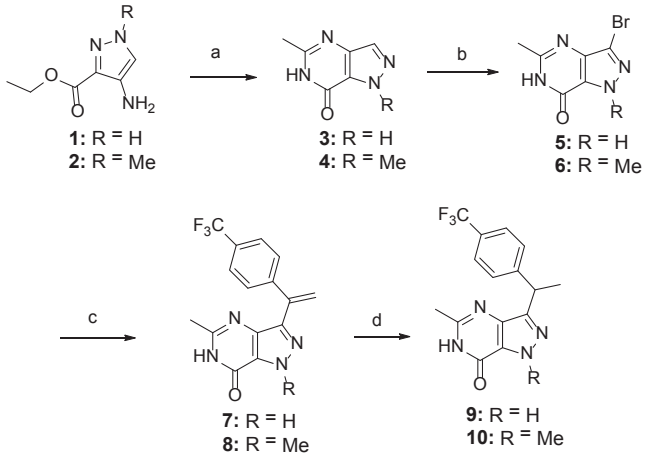

Scheme 1. (a) benzyl ethanimidiothioate hydrochloride, pyridine, 115 °C; (b) NBS, CH_3CN; (c) vinyl boronate, $Pd(OAc)_2$, sodium 3,3′,3″-phosphinetriyltribenzenesulfonate hydrate, DIPEA, DMF/H_2O; (d) H_2 (balloon), 10% Pd/C, EtOH.

and **8**. Hydrogenation of **7** and **8** using 10% Pd on carbon as catalyst yielded compounds **9** and **10,** respectively.

These initial analogs were evaluated in an *in vitro* PDE2 binding assay as well as countered screened versus PDE1 and PDE3-11. This initial data set is summarized in Table 1. Gratifyingly, the simple racemic H derivative, **9**, demonstrated promising PDE2 activity albeit with poor PDE-selectivity. The olefin compound **7** demonstrated a dramatic loss in PDE2 potency, consistent with observations in the parent pyrazolopyrimidone series.[16] Simple alkylation of the pyrazole *N1* nitrogen led to compound **10** which demonstrated a loss in PDE2 activity as well as selectivity compared to **9**. The two enantiomers of compound **9** were separated by chiral SFC to yield **11** and **11-*ent***. While compound **11** possessed a similar profile to **9**, it was clear that it would be necessary to separate any racemic compound for accurate potency and selectivity determination moving forward due to the preference for one enantiomer around the benzylic site over the other.

An X-ray co-crystal of **11** (Fig. 3) with PDE2A, revealed key interactions with active-site water molecules. The early hypothesis is that enantiomer **11-*ent*** would direct the aromatic moiety away from the hydrophobic pocket and most likely disrupt or displace one of the crucial water interactions causing a>10-fold loss in potency.

Based upon the promising results in Table 1 and the X-ray of compound **11**, efforts shifted towards the preparation of analogs bearing additional hydrogen-bonding capabilities. This design was meant to test the specific hypothesis around interactions with a non-conserved glutamine, Gln 812, which would be expected to enhance both potency and PDE-selectivity. As seen in Fig. 3, the compound forms a bidendate hydrogen bond with Gln 859 which positions the compound to have an interaction with Gln 812 through water which leads to increased PDE2 selectivity. Our hypothesis resided in the thought that increased direct interactions with Gln 812 via a direct hydrogen bonding interaction would lead to enhanced selectivity. Several methods that were employed to achieve this are shown in Schemes 2 and 3. Compound **5** could be treated with various primary bromides in the presence of K_2CO_3 to afford the *N*-alkylated cores (Scheme 2). Treatment under modified Suzuki coupling conditions using a Buchwald APhos-Pd-G3 catalyst and a vinyl boronate afforded the corresponding vinyl derivatives **14** and **15**. Hydrogenation using 10% Pd on carbon afforded the racemic mixture which was separated into the enantiopure final compounds using SFC separation in Scheme 2.

An alternative preparation of the *N*-alkylated derivatives could be achieved by treatment of compound **9** with a primary halide in the presence of K_2CO_3 to afford the final compounds **17** and **19** shown in Scheme 3.

Table 2 summarizes the SAR data for the additional linked derivatives from Schemes 2 and 3. Extension to an *N*-ethanol linker provided compound **16** which demonstrated excellent activity for PDE2 while maintaining over 450-fold selectivity versus the other PDE's tested. The enantiomeric derivative **16-*ent*** lost over an order of

Table 1

In vitro profiles of pyrazolopyrimidione derivatives **7,9–11**.

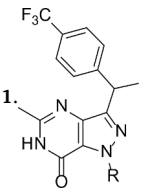

Compd	R	hPDE2 *Ki* (nM)[a]	hPDEx1-11 selctivity
9	H	27	>20
7	H	2360	nt
10	Me	70	>9
11	H	15	>22
11-*ent*	H	293	nt

[a] Values are the mean of two (n = 2) runs. See Supporting Information for assay details. [b]nt = not tested.

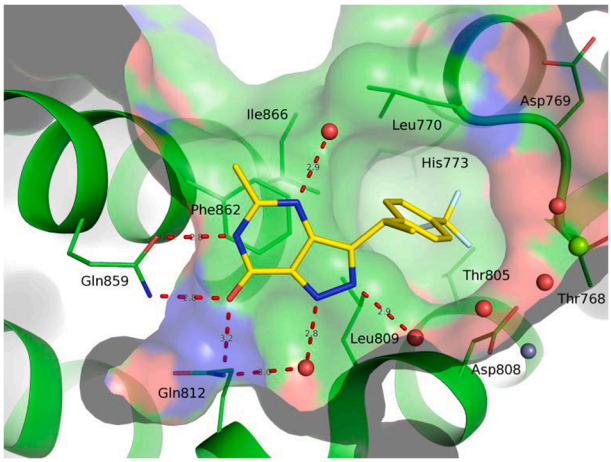

Fig. 3. X-ray crystal structure of compound **11** bound to PDE2.

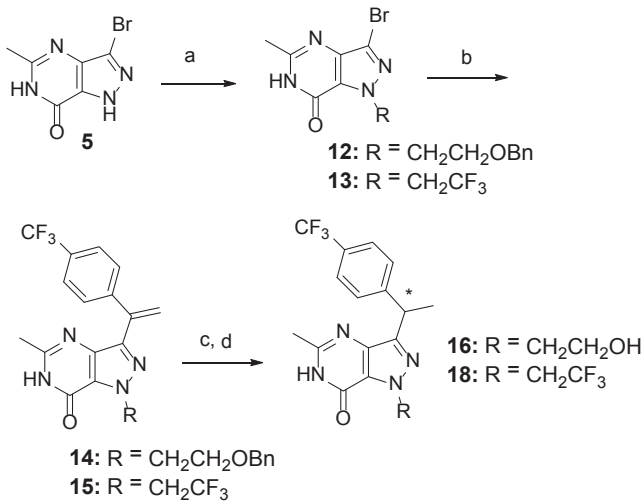

Scheme 2. (a) $BrCH_2CH_2OBn$ or $BrCH_2CF_3$, K_2CO_3, 75 °C, DMF; (b) vinyl boronate, Aphos Pd G3, 1 M K_3PO_4, NMP, 80 °C; (c) H_2 (balloon), 10% Pd/C, EtOH; (d) SFC separation.

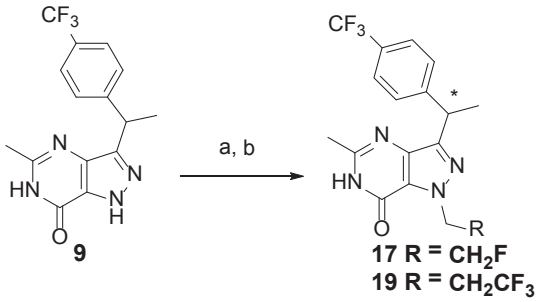

Scheme 3. (a) $BrCH_2CF_3$ or $BrCH_2CH_2CF_3$, K_2CO_3, 75 °C, DMF; (b) SFC separation.

magnitude in activity versus PDE2 in addition to exhibiting a serious erosion in selectivity versus the other PDE's (>13 only). Interestingly, the ethyl fluoro derivatives, **17** and **17-*ent***, showed very similar trends with the former compound possessing a good balance of PDE2 potency and selectivity (Table 2). The trifluoroethyl derivative **18** demonstrated reasonable PDE2 activity coupled with reduced selectivity for PDE2 (>130) while the enantiomer was not of interest. Interestingly, both of

Table 2

In vitro profiles of pyrazolopyrimidione derivatives **11, 16-19**.

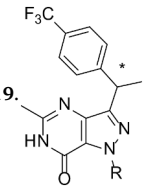

Compd	R	PDE2 *Ki* (nM)[a]	hPDEx1-11 selctivity
11	H	15	>22
11-*ent*	H	293	nt[b]
16	OH	1.7	>480
16-*ent*	OH	64.7	>13
17	F	1.8	>350
17-*ent*	F	26.8	>13
18	CF_3	7.0	>130
18-*ent*	CF_3	178	nt[b]
19	CF_3	324	nt[b]
19-*ent*	CF_3	521	nt[b]

[a] Values are the mean of two (n = 2) runs. See Supporting Information for all assay details. [b]nt = not tested.

the trifluoropropyl derivatives, **19** and **19-*ent***, showed very poor PDE2 activity shown in Table 2. As can be seen, PDE2 potency starts drifting as bulkier substituents and longer chain lengths are added. This loss in potency may be due to steric clashes of the larger substituents in the narrow pocket between Leu 809 and Gln 812. Also, the longer chain puts the substituent too far away from the important direct interact with Gln 812 which would also cause deterioration of the PDE2 potency.Table 3.

As it was evident that an additional hydrogen bonding moiety in between the inhibitor and Gln 812 enhanced PDE2 selectivity, efforts were then focused on the two optimal *N*-substituents: the terminal fluoro and hydroxyl moieties. Hydroxy ethyl and fluoro ethyl were chosen as the N1 substituent with the highest potential to participate in this additional interaction with Gln 812. Keeping these two N1 substituents constant we also sought to investigate SAR around the benzylic phenyl ring and an appropriate synthetic route was designed to accommodate these plans.

As seen in Scheme 4, the starting bromo intermediate was first alkylated with 2-benzoloxy-1-bromoethane to enable access to both the hydroxyl and fluoro analogs from a common intermediate. Heck reaction of **12** with 1-(ethyloxy)butane in ethylene glycol afforded a vinyl ether, which upon treatment with 2 M HCl gave ketone **20**. The ketone was then treated with either an aryl Grignard or an aryllithium reagent, to provide the substituted tertiary aryl alcohol. Elimination with Burgess reagent then afforded olefin **21**. Reduction of the double bond with concomitant removal of the benzyl protecting group could be achieved with 10% Pd/C in ethanol under an atmosphere of H_2. This racemic mixture was then be separated via chiral HPLC to give compounds **22**–**24**. Lastly, manipulation of the alcohol of the active enantiomers with DAST afforded fluoroethyl targets **25** and **26.**

Gratifyingly, >1000-fold selectivity was achieved by the introduction of a hydrogen-bond donating hydroxyl group forming an additional direct interaction with Gln 812. When comparing the two sub-series, it is apparent that hydroxyl substituted compounds **22** and **24** are more sensitive to arene substitution than their matched-pair fluoro analogs **25**

Table 3

In vitro profiles of pyrazolopyrimidione derivatives **22**–**26**.

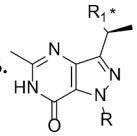

Compd	R	R_1	PDE2 Ki (nM)[a]	hPDEx1-11 selctivity
22		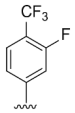	1.1	>1500
23			208	–
24		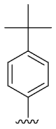	2.6	>2000
25		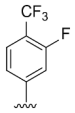	0.92	>500
26		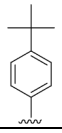	1.3	>500

[a] Values are the mean of two (n = 2) runs. See Supporting Information for all assay details. [b]nt = not tested.

and **26**. In contrast, comparison of the *para*-CF_3 compounds **16** and **17** to their matched pair containing *para*-*t*-butyl and *meta*-F, *para*-CF_3 analogs in the fluoro containing sub-series, minimal selectivity differences were observed (>350 for **17** vs > 500 for both **25**, **26** respectively). As for the hydroxyl containing compounds, a gain of 2- to 4-fold increased selectivity is observed with the analogous substitutions on the phenyl ring (>480 for **16** vs > 1000 and > 2000 for **22**, **24** respectively). One explanation for this increase in selectivity might be the better Vanderwaal interactions of the aromatic ring in the hydrophobic pocket (Ile 870 and Thr 850 residues) caused by extensive water networking with key parts of the PDE2 active site. (Fig. 4 and 5) As seen in Fig. 4, the hydroxyl substituent interaction with the non-conserved Gln812 side chain provides a rationale for enhanced selectivity.

Since compounds **22** and **26** displayed the best affinity for PDE2 and acceptable selectivity over the other PDE family members, they were both further profiled for their pharmacokinetic properties. In both Tables 4 and 5, a combined heat map and data record was added to help visualize the selectivity versus the other PDE isoforms to which green is > 500 fold selectivity, orange is between 100 and 500 fold and red is < 100 fold compared to their PDE2 potency. Compound **22** showed promising overall properties with a good rat Pharmacokinetic (PK) profile with moderate clearance and 3 h effective half-life, and also excellent selectivity on the ancillary targets (CYPs, ion channels, PXR). Compound **22** also displayed good kinetic solubility (pH = 7; 117 μM, FASSIF: 148 μM) and good passive permeability (Papp = 29.5). However, the polarity of the hydroxyl group resulted in an higher Pgp efflux ratio in both rat and human cell lines (AB:BA ratio 18.7 rat; 3.3 human). Although, *in silico* predictions of brain penetration potential, .i.e. CNS probabilistic Multiparameter Optimization (pMPO) and rat Pgp were in a favorable range (0.77 and AB:BA predicted ratio 3.2, respectively), experimental Pgp efflux ratios were observed to be significantly higher than the predicted values limiting consideration of these compounds for further advancement. The fluoro analog **26** was also predicted to have favorable *in silico* brain penetration properties (CNS pMPO: 0.76, Pgp: 1.0) but since **26** has one less hydrogen bond donor and acceptor in the

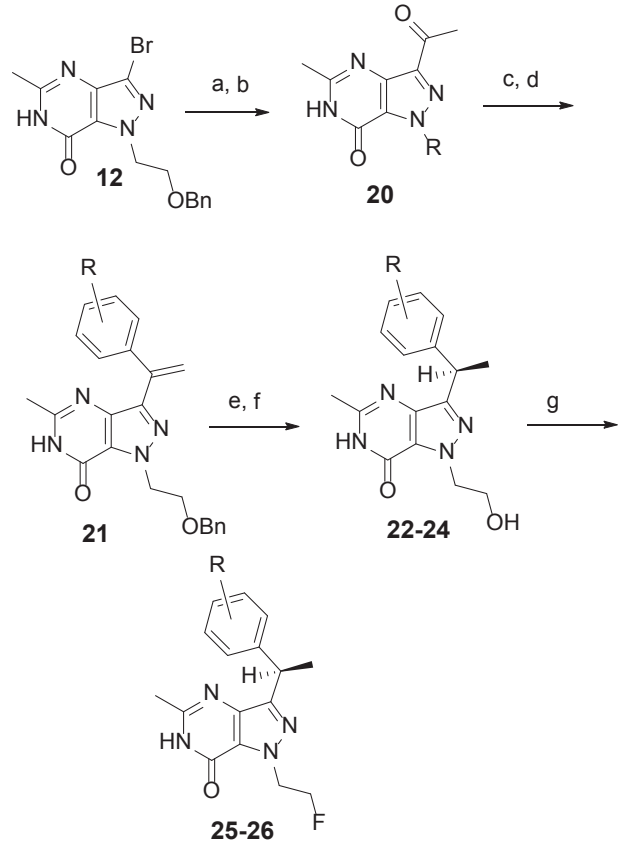

Scheme 4. (a) 1-(ethenyloxy)butane, DPPP, $Pd(OAc)_2$, Et_3N, ethylene glycol, 145 °C; (b) 2 M HCl, THF, rt; (c), ArLi or ArMgBr, THF, −78 °C; (d) Burgess reagent, toluene, 110 °C: (e) H_2 (balloon), 10% Pd/C, EtOH; (f) Chiral HPLC or SFC separation; (g) DAST, CH_2Cl_2, rt.

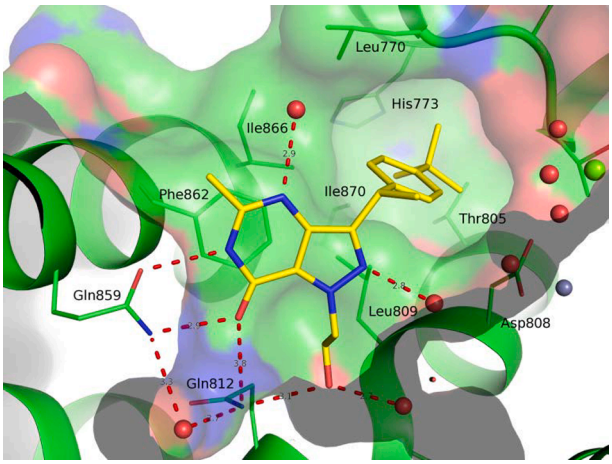

Fig. 4. X-ray crystal structure of compound **24** bound to PDE2.

structure, it was hoped it would have reduced susceptibility to act as a Pgp efflux substrate. This was confirmed experimentally and compound **26** was found not to be a substrate for Pgp efflux; 1.3 respectively. In addition to that, CNS penetration potential of compound **26** displayed good cell permeability, and a relatively clean ancillary profile, with good FASSIF solubility (177 μM) and as such was chosen for additional profiling in *in vivo* pharmacokinetic studies. Unfortunately, compound **26** exhibited high plasma clearence and a relatively short half-life of 0.8 h in rat. Efforts to optimize pharmacokinetic profile of this series will be

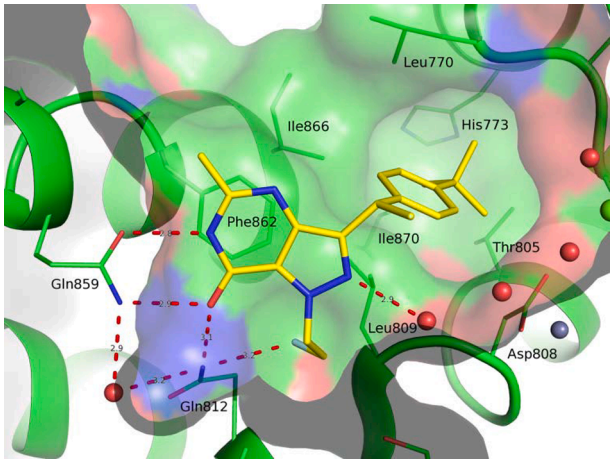

Fig. 5. X-ray crystal structure of compound **26** bound to PDE2.

Table 4

Full physicochemical summary of compound **22**.

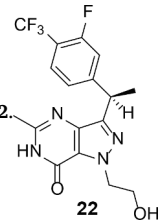

PDE 2-h IC_{50}: 1.1 nM
PDE(1-11) selectivity:

PDE:	1	3	4	5	6	7	8	9	10	11
μM:	> 60	1.8	3.5	23	27	> 75	> 50	> 50	18	6.2

Pharmacokinetics Rat		Kinetic Solubility rat (μM)	
Clp: (ml/min/kg) 24	24	pH 2	117
t1/2: (h)	3.1	FASSIF	148
MRT: (h)	2.5	pH 7	115

Pgp efflux		Metabolic stability	
Rat BA/AB ratio	18.7	Hum heps	Int Cl: 11.4
Human BA/AB ratio	3.3	Rat hep	Int Cl: 137.4
Control	0.8		

Ancillary activity		PPB (F_u)	
CYP inhibition		Rat	4.9%
2D6	>50 μM	Rhesus	3.5%
3A4	44 μM	Human	3.0%
2C9	>50 μM		
Ion Channels	9.6–30 μM		
hPXR	16%@10 μM		

the subject of future manuscripts.

In conclusion, we were able to identify a new core motif via a "flip" (isostere) of the pyrazole of a core pyrazolopyrimidinone described previously in our labs. After establishing robust chemistry to synthesize the first set of novel *N*1-substituted pyrazolopyrimidinones, we quickly established the viability of the new core motif with unique potent PDE2 inhibitors (**9**, **10**, and **11**). With the aid of molecular modeling and X-ray crystallography, compound **11** was futher derivatized to optimize new compound designs to afford enhanced selectivity and PDE2 potency. Preparation of analogs bearing additional H-bonding capabilities were targeted based on the hypothesis that the extensive water and hydrogen bonding network to key amino acids in the PDE2 active site would boost potency and PDE2 selectivity. Finally, we further identified two

Table 5

Full physicochemical summary of compound 26.

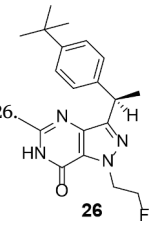

PDE 2-h IC_{50}: 1.3 nM
PDE(1-11) selectivity:

PDE:	1	3	4	5	6	7	8	9	10	11
μM:	> 60	5.7	3.3	21	11	> 75	>50	> 50	5.8	0.6

Pharmacokinetics rat		Kinetic Solubility rat (μM)	
Clp: (ml/min/kg)	49	pH 2	60
t1/2: (h)	1.4	FASSIF	177
MRT: (h)	0.8	pH 7	20

Pgp efflux		Metabolic stability	
Rat BA/AB ratio	1.4	Hum heps	Int Cl: 16.4
Human BA/AB ratio	0.6	Rat heps	Int Cl: 54.2
Control	0.7		

Ancillary activity		PPB (F_u)	
CYP inhibition		Rat	1.4%
2D6	>50 μM	Rhesus	1.6%
3A4	>50 μM	Human	0.9%
2C9	>50 μM		
Ion Channels	17–30μM		
hPXR	45%@10 μM		

compounds which were profiled for pharmacokinetic properties. Compounds **22** and **26** both demonstrated excellent PDE2 potency (1.1 and 1.3 nM respectively) and PDE-family selectivity (>400 fold), good cell permeability, and favorable ancillary target profiles. Additionally, compound **26** proved to fit most of the set criteria to commit to future ongoing studies to access its potential for further development.

Declaration of Competing Interest

The authors declare that they have no known competing financial interests or personal relationships that could have appeared to influence the work reported in this paper.

Acknowledgment

The authors would like to thank Santhosh Neelamkavil for his helpful review and insights.

References

1 Maurice DH, Ke H, Ahmad F, Wang Y, Chung J, Manganiello VC. *Nat Rev Drug Discovery*. 2014;13:290.
2 Francis SH, Blount MA, Corbin JD. *Physiol Rev*. 2011;91:651.
3 Frey U, Huang YY, Kandel ER. *Science*. 1993;260:1661.
4 Son H, Lu YF, Zhuo M, Arancio O, Kandel ER. *Learn Mem*. 1998;5:231.
5 Bernabeau R, Schmitz P, Faillace MP, Izquierdo I, Medina JH. *NeuroReport*. 1996;7:585.
6 Martinez SE, Wu AY, Glavas NA, et al. *PNAS*. 2002;99:13260.
7 Lakics V, Karran EH, Boess FR. *Neuropharmacology*. 2010;59:367.
8 (a) Gomez L, Breitenbucher JG. *Bioorg Med Chem Lett*. 2013;23:6522.(b) Jorgensen M, Kehler J, Langgard M, Svenstrup N, Tagmose L. *Ann Reports in Med Chem*. 2013;48:37.
9 Bayer compound: Boess, F. G.; Hendrix, M.; van der Staay, J.-F.; Erb, C.; Schreiber, R.; van Staveren, W.; deVente, J.; Prickaerts, J.; Blokland, A.; Koenig, C. Neuropharmacology 2004, 47, 1081.
10 Evotec compound: Abarghaz, M.; Biondi, S.; Duranton, J.; Limanton, E.; Mondadori, C.; Wagner, P. WO2005063723.

11 TAK-915: Mikami, Satashi; Nakamura, Shinji; Ashizawa, Tomoko; Nomura, Izumi; Kawasaki, Masanori; Sasaki, Shigekazu; Oki, Hideyuki; Kokubo, Hironori; Hoffman, Isaac D.; Zou, Hua; Uchiyama, Noriko; Nakashima, Kosuke; Kamiguchi, Naomi; Imada, Haruka; Suzuki, Noriko; Iwashita, Hiroki; Taniguchi, Takahiko. J. Med. Chem. 2017, 60(18), 7677.
12 Janssen compound:(a) Rombouts, F. J. R.; Tresadern, G.; Buijnsters, P.; Langlois, X.; Tovar, F.; Steinbrecher, T. B.; Vanhoof, G.; Somers, M,; Andres, J.-I.; Trabanco, A. A. ACS Med. Chem. Lett. 2015, 6, 282. (b) Buijnsters, P.; De Angelis, M.; Langlois, X.; Rombouts, F. J. R.; Sanderson, W.; Tresadern, G.; Ritchie, A.; Trabanco, A. A.; VanHoof, G.; Roosbroeck, Y. V.; Andres, A. A. ACS Med. Chem. Lett. 2014, 5, 1049.
13 Pfizer PF-099: (a) Helal, C. J.; Chappie, T. A.; Humphrey, J. M.; WO2012168817. (b) Helal, C. J.; Chappie, T. A.; Humphrey, J. M.; Verhoest, P. R.; Yang, E. US20120214791.
14 Other Pfizer core: (a) Plummer, M. S.; Cornicelli, J.; Roark, H.; Skalitzky, D. J.; Stankovic, C. J.; Bove, S.; Pandit, J.; Goodman, A.; Hicks, J.; Shahripour, A.; Beidler, D.; Lu, X. K.; Sanchez, B.; Whitehead, C.; Sarver, R.; Braden, T.; Gowan, R.; Shen, X. Q.; Welch, K.; Ogden, A.; Sadagopan, N.; Baum, H.; Miller, H.; Banotai, C.; Spessard, C.; Lightle, S. Bioorg, Med. Chem. Lett. 2013, 23, 3438. (b) Plummer, M. S.; Cornicelli, J.; Roark, H.; Skalitzky, D. J.; Stankovic, C. J.; Bove, S.; Pandit, J.; Goodman, A.; Hicks, J.; Shahripour, A.; Beidler, D.; Lu, X. K.; Sanchez, B.; Whitehead, C.; Sarver, R.; Braden, T.; Gowan, R.; Shen, X. Q.; Welch, K.; Ogden, A.; Sadagopan, N.; Baum, H.; Miller, H.; Banotai, C.; Spessard, C.; Lightle, S. Bioorg, Med. Chem. Lett. 2013, 23, 3443.
15 Forster, Ashley B.; Abeywickrema, Pravien; Bunda, Jaime; Cox. Christopher D.; Cabalu, Tamara D.; Egbertson, Melissa; Fay, John; Getty, Krista; Hall, Dawn; Kornienko, Maria; Lu, Jun; Parthasarathy, Gopal; Reid, John; Sharma, Sujata; Shipe, William D.; Smith, Sean M.; Soisson, Stephen; Stachel, Shawn J.; Su, Hua-Poo; Wang, Deping; Berger, Richard. Bioorg, Med. Chem. Lett. 2017, 27, 5167.
16 Stachel Shawn J, Berger Richard, Nomland Ashley B, et al. *ACS Med Chem Lett.* 2018; 9:815.